Quadratic magnetooptic effects in orthoferrites

E. A. Gan'shina, A. V. Zenkov, G. S. Krinchik, A. S. Moskvin, and A. Yu. Trifonov

M. V. Lomonosov State University, Moscow

(Submitted 5 July 1990)
Zh. Eksp. Teor. Fiz. **99**, 274–285 (January 1991)

The spectral dependences of the orientational magnetooptic effect in $TmFeO_3$, $HoFeO_3$, and $DyFeO_3$ were determined in the photon energy range 2–4 eV. The results were then used to calculate the quadratic (in respect of the magnetization) corrections to the diagonal permittivity-tensor $\Delta\varepsilon_{ii}$ components responsible for this magnetooptic effect. The spectra of $\Delta\varepsilon_{ii}(\omega)$ were anisotropic and were characterized by a strong dispersion. Theoretical estimates of the contributions of the various mechanisms of the quadratic magnetooptic effects, obtained assuming the dominant role of charge-transfer transitions in octahedral FeO_6^{9-} complexes, demonstrated that only the magnetooptic mechanism combining both the macroscopic magnetostriction with the latent displacements of ions in the sublattices can account for the large magnitude and anisotropy of the quadratic magnetooptic effects.

INTRODUCTION

Investigations of the quadratic (in respect of the magnetization), i.e., even magnetooptic effects in ferromagnets, ferrimagnets, and antiferromagnets have shown that the magnetic linear birefringence (MLBR) is anomalously strong in these materials and in some cases can even exceed the linear (odd) magnetooptic effects. For example, a strong MLBR of α-Fe_2O_3 was first observed in the infrared range[1] and then determined at visible and ultraviolet wavelengths.[2] It was suggested in Ref. 2 that the large magnitude of the quadratic magnetooptic effects, observed directly in the region of the fundamental transition frequencies, was responsible for the strong MLBR in the transparency range. The high values of the MLBR were reported also for easy-plane weak ferromagnets $MnCO_3$ and $CoCO_3$ (Refs. 3 and 4) and for antiferromagnets[5] (the fullest review of the experimental data on the MLBR in the transparency range and a theoretical analysis of its mechanisms can be found in Ref. 6).

Large values of the MLBR and of the dichroism are observed in the region of absorption bands of magnetically active ions in crystals. Anisotropic effects of this type, which are due to the dependence of the energy of the excited levels of Eu^{3+} on the orientation of the magnetization vector in a crystal, had been reported for the $^7F_0$–$^7F_4$ transition in $Eu_3Fe_5O_{12}$ (Refs. 7 and 8). A record value of the MLBR, of the order of the natural birefringence of crystals, was $\Delta n = 2\times 10^{-2}$ reported for EuSe ($\lambda = 0.725$ μm, $T = 4.2$ K) in Ref. 9.

The MLBR for the orthoferrite $YFeO_3$ was determined in the transparency range at $\lambda = 0.6328$ μm in Ref. 10 and was analyzed theoretically in Ref. 11 using a simple deformation model in which the relationship between the polarizability of the FeO_6^{9-} complexes due to their deformation (caused by magnetostrictive and magnetoelastic contributions) was considered. The magnetoelastic contribution was due to latent displacements of the sublattices. The problem of the need to allow for the latent displacements had been formulated earlier in attempts to explain the strong MLBR in easy-plane weak ferromagnets, in antiferromagnets, and in iron garnets, since a theoretical estimate of the value of Δn deduced from the known elastooptic constants gave values two orders of magnitude less than those found experimentally.[6]

Investigations of the spectral dependences of the quadratic magnetooptic effects in the region of the fundamental optical transition frequencies can give valuable information on the mechanisms responsible for these effects. To the best of our knowledge, there have been no such measurements in the case of rare-earth orthoferrites.

The hypothesis of charge-transfer transitions in octahedral FeO_6^{9-} complexes had been used successfully to account for the linear magnetooptic effects in paramagnetic and single-sublattice garnets, in iron garnets, and in weak ferromagnets.[21,13] It seemed of interest to study the contributions of such transitions to the quadratic magnetooptic effects in the case of rare-earth orthoferrites and to analyze in this specific case the physical mechanisms responsible for the anomalously strong quadratic (even) magnetooptic effects in magnetically ordered crystals.

We shall report the results of experimental and theoretical investigations of the quadratic magnetooptic effects observed in the region of spin-reorientation Γ_4–Γ_2 transitions in orthoferrites $TmFeO_3$ and $HoFeO_3$, and of Γ_4–Γ_1 transitions in $DyFeO_3$ at wavelengths corresponding to the photon energy range 2–4 eV.

1. SAMPLES AND EXPERIMENTAL METHODS

We used thulium and holmium orthoferrite samples polished along (010) planes and also a sample of $DyFeO_3$ polished along a (110) plane. All the samples were grown by the floating zone method involving radiation heating.

The spectra of quadratic corrections to the diagonal elements of the permittivity tensor were deduced from measurements of the orientational magnetooptic effect, representing a quadratic (in respect of the magnetization) change in the intensity of light reflected from a sample as a result of a change in the spin orientation. We described the spin system of orthoferrites in terms of the ferromagnetic **M** and antiferromagnetic **L** vectors. Direct experimental measurements were made of the quantity $\delta = (I_1 - I_2)/I_0$, where I_1 and I_2 are the intensities of light reflected from a sample for different orientations of the vectors **M** and **L**, whereas I_0 is the

 0038-5646/91/010154-07$03.00

intensity of light reflected in the demagnetized state. It should be pointed out that δ has components which are linear and quadratic in respect of the magnetization. The linear component represents the equatorial Kerr effect, whereas the quadratic component describes the orientational magnetooptic effect. They can be separated by the method of unipolar magnetization:

$$\delta(H) = \delta_l + \delta_q,\ \delta(-H) = -\delta_l + \delta_q.$$

Such measurements of the orientational magnetooptic effect can be carried out particularly conveniently at temperatures close to the region of spin-reorientation transitions because in other cases the anisotropy fields in the $\Gamma_2(M_xL_z)$ and $\Gamma_4(M_zL_x)$ phases are very high and external fields of the order of tens of kilo-oersted are needed to measure the orientational magnetooptic effect. A spin reorientation of the $\Gamma_4(M_zL_x)$–$\Gamma_{24}(M_xM_zL_xL_z)$–$\Gamma_2(M_xL_z)$ type occurs in $TMFeO_3$ and $HoFeO_3$. In the case of the intermediate phase Γ_{24} it is sufficient to apply an external field of 5 kOe to rotate the vectors **M** and **L** through $\theta \sim 30°$. In the case of the $\Gamma_4(M_zL_x)$–$\Gamma_1(L_y)$ Morin transition in $DyFeO_7$ an external field applied along the *c* axis gives rise to an intermediate phase $\Gamma_{14}(M_zL_xL_y)$. An increase of the external magnetic field induces a reorientation of the antiferromagnetic vector **L** in the *ab* plane of this intermediate phase.[14] There is no change in the direction of the vector **M**, but only its modulus is affected. Nevertheless, such a situation also gives rise to the orientational magnetooptic effect.

Our measurements were carried out using three different orientations of the samples. The relative orientations of the crystal axes, of the direction of light, and of the applied magnetic field are shown for these cases in Fig. 1. In the case of orthoferrites $TmFeO_3$ and $HoFeO_3$ the measurements were carried out using orientations I and II (Figs. 1a and 1b, respectively), whereas in the case of $DyFeO_3$ the orientation III was that shown in Fig. 1c.

An automated magnetooptic system made it possible to carry out measurements in the photon energy range 1.5–4.5 eV using light incident at angles of 60–75° in magnetic fields up to 5 kOe. The smallest detectable change in the effect was 10^{-5}. Low-temperature measurements were carried out in a continuous-flow optical helium cryostat where the temperature could be varied from 7 to 297 K.

The relationship between the orientational magnetooptic effect and the components of the permittivity tensor had been investigated earlier[15] and in the case of the quadratic (in respect of the magnetization) effect the following expressions were obtained there for the *s* and *p* components subject to the condition $|\varepsilon| \gg \sin^2\varphi$:

$$\delta_s = 2\cos\varphi\,\mathrm{Re}\left\{\frac{\Delta\varepsilon_s}{(\varepsilon-1)(\varepsilon-\sin^2\varphi)^{1/2}}\right\}, \quad (1)$$

$$\delta_p = -2\cos\varphi\,\mathrm{Re}\left\{\frac{\Delta\varepsilon_p(\varepsilon-\sin^2\varphi)^{1/2}}{(\varepsilon-1)(\varepsilon\cos^2\varphi-\sin^2\varphi)}\right\}. \quad (2)$$

Here, ε is the nonmagnetic part of the tensor [we shall ignore the relatively small ($\Delta\varepsilon/\varepsilon \sim 10^{-2}$) natural birefringence], whereas $\Delta\varepsilon_s$ and $\Delta\varepsilon_p$ are the changes in the permittivity tensor components due to rotation of the magnetization vector. When measurements were made in the (010) plane

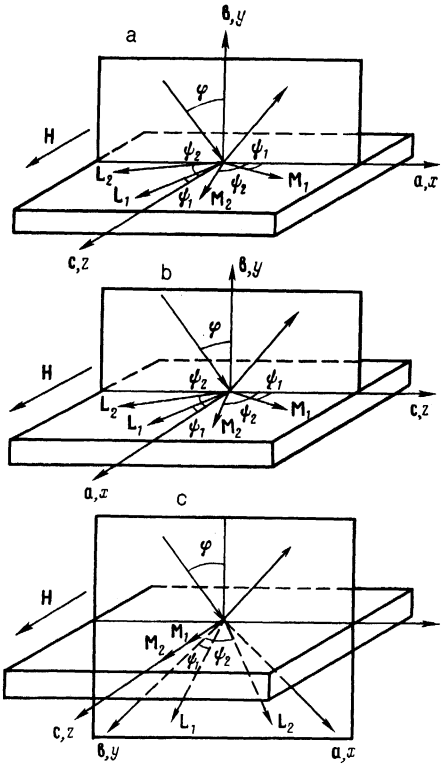

FIG. 1. Schematic representation of the relative orientations of the crystal axes, of the direction of light, and of the magnetic field used in experimental studies of the orientational magnetooptic effect: a) orientation I; b) orientation II; c) orientation III.

($HoFeO_3$ and $TmFeO_3$) in the orientation II, it was found that these components were $\Delta\varepsilon_s = \Delta\varepsilon_{xx}$ and $\Delta\varepsilon_p = \Delta\varepsilon_{zz}$, whereas in the orientation I they were $\Delta\varepsilon_s = \Delta\varepsilon_{zz}$ and $\Delta\varepsilon_p = \Delta\varepsilon_{xx}$. When measurements were made in the (110) plane ($DyFeO_3$, orientation III), the components were given by $\Delta\varepsilon_s = \Delta\varepsilon_{zz}$ and $\Delta\varepsilon_p = \frac{1}{2}\Delta(\varepsilon_{xx} + \varepsilon_{yy} + \varepsilon_{xy} + \varepsilon_{yx})$. It is clear from Eqs. (1) and (2) that the maximum magnetooptic effect can be observed for a *p* component in the region of the Brewster angle; therefore, all the experiments were carried out by us only for the *p* component.

In real experiments the reorientation of the vectors **M** and **L** was by an angle $\vartheta = \psi_2 - \psi_1 \neq 90°$, where ψ is the angle between the vector **L** and the **c** axis in the orientation I, between this vector and the **a** axis in the orientation II, and between the same vector and the **b** axis in the orientation III (see Fig. 1). The value of $\Delta\varepsilon_p$ corresponding to rotation of **L** from $\psi_1 = 0°$ to $\psi_2 = 90°$ was obtained by multiplying additionally the component $\Delta\varepsilon_p$ calculated from the experimental data with the aid of Eq. (2) by a coefficient

$$K = \frac{\delta_{\max}^2}{2(\delta_l^2 + \delta(\psi_1)\delta_l}, \quad (3)$$

where δ_l is the linear component of the effect on reorientation of **L** from ψ_1 to ψ_2; $\delta_{\max}$ is the equatorial Kerr effect for $\psi = 90°$, i.e., for the Γ_4 phase in the case of the orientations I and III, and for the Γ_2 phase in the case of the orientation II; $\delta(\psi_1)$ is the equatorial Kerr effect corresponding to the spontaneous magnetization at the temperature at which the orientational magnetooptic effect was measured. The value

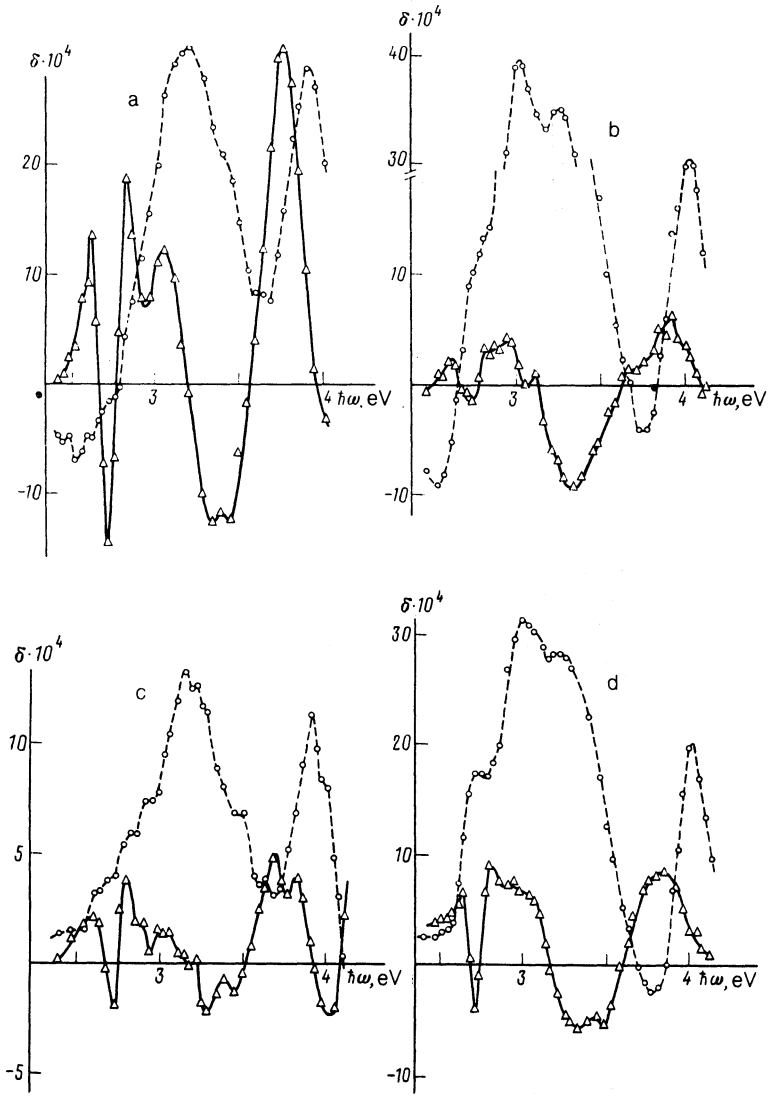

FIG. 2. Spectral dependences of the experimentally observed quantity $\delta = \delta_l + \delta_q$; the triangles and the continuous curves represent δ_q (orientational magnetooptic effect); the circles and the dashed curves represent δ_l (linear component representing the equatorial Kerr effect). a) $HoFeO_3$, $\mathbf{H}\|\mathbf{a}$, $T = 63$ K, $\varphi = 67.5°$, $\vartheta \approx 26.5°$; b) $TmFeO_3$, $\mathbf{H}\|\mathbf{c}$, $T = 80$ K, $\varphi = 67°$, $\vartheta \approx 31°$; c) $TmFeO_3$, $\mathbf{H}\|\mathbf{a}$, $T = 95$ K, $\varphi = 64.5°$, $\vartheta \approx 13°$; d) $DyFeO_3$, $\mathbf{H}\|\mathbf{c}$, $T = 25$ K, $\varphi = 64°$, $\vartheta \approx 24°$.

of $\delta(\psi_1)$ was found experimentally in the weakest field sufficient to reverse abruptly the magnetization of the sample, i.e., to rotate it by 180° ($H \sim 200$ Oe) without rotation of the vector **L**.

2. EXPERIMENTAL RESULTS

Figure 2 shows the orientational magnetooptic effect spectra recorded for rare-earth orthoferrites investigated by us: in the case of $TmFeO_3$ this was done for two different orientations (Figs. 2b and 2c); in the case of $HoFeO_3$ the spectra were obtained for $\mathbf{H}\|\mathbf{a}$ (a) and in the case of $DyFeO_3$ this was done for $\mathbf{H}\|\mathbf{c}$. The magnitude of the observed effect depended on the angle ϑ representing rotation of the vector **L**, which could be judged on the basis of the linear component of the observed effect, and also by a dashed curve shown in all the figures. The spectrum of the orientational magnetooptic effect in $HoFeO_3$ was not obtained for the $\mathbf{H}\|\mathbf{c}$ configuration, because the smallness of the value of ϑ for this orientation prevented measurements with a sufficient degree of precision.

The experimental results were substituted in Eqs. (2) and (3) to calculate the value of $\Delta\varepsilon_p$ corresponding to a rotation of the vector by 90°. The spectra obtained in this way are plotted in Figs. 3 and 4.

The relationship between the quadratic (in respect of the magnetization) part of the tensor $\hat{\varepsilon}$ and the components of the vectors **M** and **L** can generally be written in the form[16]

$$\varepsilon_{ij}^{q} = A_{ijkl}M_kM_l + B_{ijkl}L_kL_l + C_{ijkl}M_kL_l. \qquad (4)$$

Allowing for the specific form of the tensors A, B, and C for orthoferrites,[17] we can obtain an expression for $\Delta\varepsilon_p$ corresponding to complete rotation of vectors **M** and **L** by 90° from the phase $\Gamma_2(M_xL_z)$ to the phase $\Gamma_4(M_zL_x)$:

$$\Delta\varepsilon_{xx} = (A_{xxzz} - A_{xxxx})M^2 + (B_{xxxx} - B_{xxzz})L^2 - (C_{xxzz} + C_{xzxz})ML,$$
$$\Delta\varepsilon_{zz} = (A_{zzxx} - A_{zzzz})M^2 + (B_{zzzz} - B_{zzxx})L^2 - (C_{zzzx} + C_{zxzz})ML.$$

The expression for $\Delta\varepsilon_p$ applicable to $DyFeO_3$ [(110) plane, $\mathbf{H}\|\mathbf{c}$] is quite complex and will not be given here.

3. CHARGE-TRANSFER TRANSITIONS AND OPTICAL ANISOTROPY OF FERRITES

The electron configuration of the ground state of the FeO_6^{9-} complexes, which are the main optical centers in

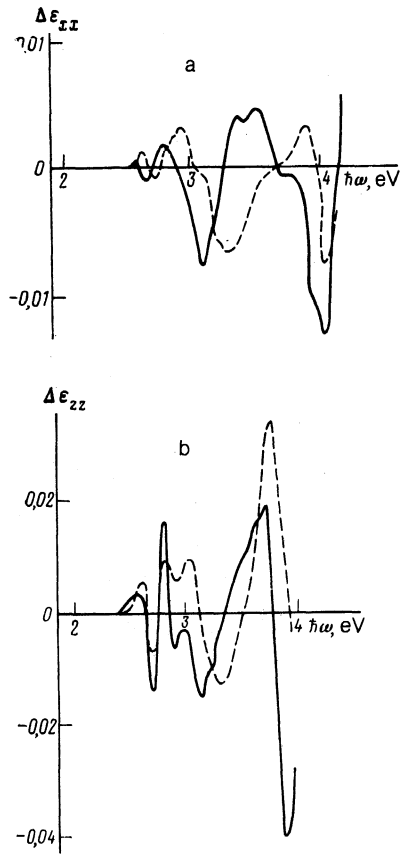

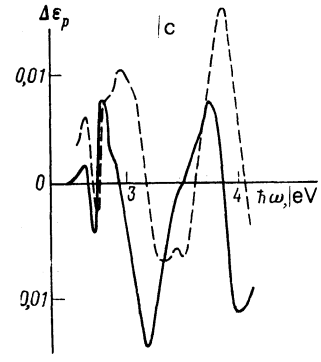

FIG. 3. Spectrum of the quadratic (in respect of the magnetization) component of the permittivity tensor $\Delta\varepsilon_p$. The continuous curves represent $\mathrm{Re}(\Delta\varepsilon_p)$, whereas the dashed curves represent $\mathrm{Im}(\Delta\varepsilon_p)$. a) $TmFeO_3$, $\Delta\varepsilon_p = \Delta\varepsilon_{xx}$; b) $HoFeO_3$, $\Delta\varepsilon_p = \Delta\varepsilon_{zz}$; c) $DyFeO_3$, $\Delta\varepsilon_p = \frac{1}{2}\Delta(\varepsilon_{xx} + \varepsilon_{yy} + \varepsilon_{xy} + \varepsilon_{yx})$.

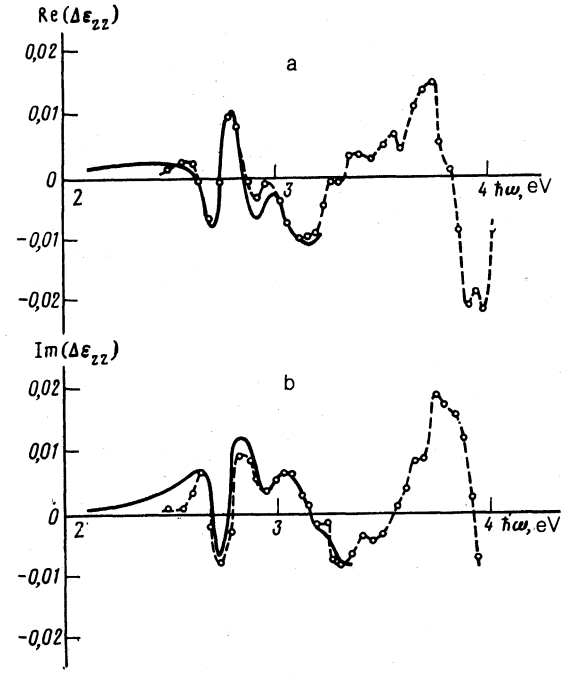

FIG. 4. Spectral dependences of the quadratic (in respect of the magnetization) component of the permittivity tensor $\Delta\varepsilon_{zz}$ of orthoferrite $TmFeO_3$. The experimental results are represented by circles and the dashed curves and the model analysis is represented by the continuous curves. a) $\mathrm{Re}(\Delta\varepsilon_{zz})$; b) $\mathrm{Im}(\Delta\varepsilon_{zz})$.

orthoferrites, is characterized by the existence of several filled valence molecular orbitals of the O_{2p} type and also of half-filled t_{2g} and e_g orbitals of the $3d$ type (Ref. 18). The transition of an electron from O^{2-} to Fe^{3+} produces a charge-transfer configuration of the $\tilde{\gamma}_{2p}t_{2g}^4e_g^2$ type (γ_{2p}–t_{2g} transfer) or of the $\tilde{\gamma}_{2p}t_{2g}^3e_g^3$ type (γ_{2p}–e_g transfer), where γ_{2p} represents a $2p$ hole in an anion molecular orbital core.

In accordance with the parity, spin, and quasimomentum selection rules, electric-dipole transitions from the ground state $(t_{2g}^3e_g^2)^6A_{1g}$ of an FeO_6^{9-} complex are allowed only to the terms $^6T_{1u}$ of charge-transfer configurations of the $\tilde{\gamma}_{2p}(t_{2g}^4e_g^2{:}^5T_{2g})$ or $\tilde{\gamma}_{2p}(t_{2g}^3e_g^3{:}^5E_g)$ types, where $\gamma_{2p} = t_{2u}, t_{1u}(\pi), t_{1u}(\sigma)$. We therefore have six electric-dipole charge-transfer transitions $^6A_{1g}$–$^6T_{1u}$ associated with one-electron transitions $t_{2u}, t_{1u}(\pi), t_{1u}(\sigma)$–$t_{2g}$ (their calculated energies are 3.1, 3.9, and 5.1 eV, respectively—see Ref. 18) and $t_{2u}, t_{1u}(\pi), t_{1u}(\sigma)$–$e_g$ (calculated energies 4.4, 5.3, and 6.4 eV, respectively (see Ref. 18). In addition to the allowed $^6A_{1g}$–$^6T_{1u}$ transitions, there may be also numerous forbidden charge-transfer transitions among which we should mention "satellites" of the allowed transitions whose final states are characterized by different terms with the same electron configurations. These are transitions of the $^6A_{1g}$–$^6\Gamma_u$ type (where $\Gamma = A_1, A_2, E, T_2$), forbidden by the quasimomentum selection rules, and transitions of the $^6A_{1g}$–$^4\Gamma_u$ type (where $\Gamma = A_1, A_2, E, T_1, T_2$), forbidden by the spin and quasimomentum rules (with the exception of

the case when $\Gamma = T_1$). The forbiddenness of such transitions is lifted by the action of a low-symmetry crystal field (LCF) and/or the spin–orbit interaction, or also by the exchange with the adjacent complexes.

All these interactions are of fundamental importance in determination of the contribution of the octahedral FeO_6^{9-} complexes to the optical anisotropy. In the case of a specific $^6T_{1u}$ term the LCF and the spin–orbit interaction can be represented by the following effective operators:

$$V_{\text{LCF}} = \sum_{ij} B_{ij}\left[L_{ij} - \frac{1}{3}L(L+1)\delta_{ij}\right], \tag{5}$$

$$V_{so} = \lambda \mathbf{LS}, \tag{6}$$

where $\mathbf{L}$ is the effective orbital moment of the T_1 term ($L = 1$); $L_{ij} = (L_iL_j + L_jL_i)/2$; B_{ij} is a symmetric matrix of the LCF parameters; λ is the effective spin–orbit coupling constant. The orbitally anisotropic part of the exchange interaction of the $^6T_{1u}$ term of an octahedral complex 1 with an adjacent octahedral complex 2, which is in the ground $^6A_{1g}$ state, can be reduced to Eq. (5) by the substitution

$$B_{ij} \to B_{ij}^{(0)} + B_{ij}^{(1)}(\mathbf{S}_1\mathbf{S}_2). \tag{7}$$

A microscopic calculation of the polarizability $\hat{\alpha}$ of complexes of the FeO_6^{9-} type can be made using the familiar Kramers–Heisenberg formula,[19] which has the following form for the symmetric part of the tensor $\hat{\alpha}$:

$$\alpha_{kl} = \frac{1}{\hbar}\sum_{ij}\rho_i\langle i|d_k|j\rangle\langle j|d_l|i\rangle F(\omega, \omega_{ij}), \tag{8}$$

where

$$F(\omega, \omega_{ij}) = \frac{2\omega_{ij}}{(\omega + i\Gamma_{ij})^2 - \omega_{ij}^2}. \tag{9}$$

Here, $\langle i|d|j\rangle$ represents the matrix elements of the electric dipole moment, ρ_i is the statistical weight of the initial state $|i\rangle$, ω_{ij} is the frequency of the $|i\rangle \to |j\rangle$, transition, and Γ_{ij} is the half-width of the line representing this transition.

In practice, the polarizability is calculated using perturbation theory and selecting as the zeroth approximation, the energies and wave functions of $^{2S+1}\Gamma$ terms of an ideal FeO_6^{9-} octahedral complex and distinguishing several contributions to the polarizability: a) a contribution associated with an allowance for the orbital splitting of the final states $|j\rangle$ under the action of various perturbations; b) a splitting contribution governed by the admixture to the $|j\rangle$ states of other states under the influence of various perturbations; c) combined contributions which appear in the second and higher orders of perturbation theory and are related to simultaneous allowance for the action of various mechanisms referred to above.

For example, in the first approximation, the contribution of the splitting of the $^6T_{1u}$ terms of an FeO_6^{9-} complex under the influence of the LCF into the components of the tensor can be represented as follows:

$$\alpha_{kl} = \frac{1}{2}\sum_{j=^6T_{1u}} \frac{e^2 f_j}{\hbar m_e \omega_{0j}} B_{kl}^{(j)} \frac{\partial F(\omega, \omega_{0j})}{\partial \omega_{0j}}, \tag{10}$$

where f_j is the oscillator strength of the $^6A_{1g} \to |j\rangle$ transition and B_{kl} are the parameters of the LCF.

The spin–orbit splitting of the $^6T_{1u}$ terms of an FeO_6^{9-} complex contributes to the symmetric part of the polarizability tensor only in the second order of perturbation theory:

$$\alpha_{kl} = \frac{1}{2\cdot 3^{1/2}}\sum_{j=^6T_{1u}} \frac{e^2(\lambda^j)^2 f_j}{\hbar^2 m_e \omega_{0j}}\left\langle S_{kl} - \frac{1}{3}S(S+1)\delta_{kl}\right\rangle \frac{\partial^2 F(\omega, \omega_{0j})}{\partial \omega_{0j}^2}, \tag{11}$$

where λ^j is the spin–orbit coupling constant for the state $|j\rangle$.

On the whole, the spectral dependence of the contribution of charge-transfer transitions to the components of the symmetric part of the polarizability tensor can be approximated by

$$\alpha_{kl} = \sum_{S\Gamma} A_{kl}^{S\Gamma} F(\omega, \omega_{S\Gamma}) + B_{kl}^{S\Gamma} F'(\omega, \omega_{S\Gamma}) + C_{kl}^{S\Gamma} F''(\omega, \omega_{S\Gamma}), \tag{12}$$

which probably makes it possible to allow for all the main optical anisotropy mechanisms. The sum over S and Γ in Eq. (12) includes the allowed $^6A_{1g}$–$^6T_{1u}$ and forbidden charge-transfer transitions.

An analysis of the experimental data on the optical anisotropy and on the quadratic magnetooptic effect, made on the basis of Eq. (12), should naturally agree with the data on the optical absorption and on the spectral dependences of the circular magnetooptic effects. In particular, this applies to the frequencies of the $^6A_{1g}$–$^{2S+1}\Gamma_u$ transitions, the line half-widths Γ_j, and the oscillator strengths f_j.

Unfortunately, there are no published experimental data on the optical anisotropy of ferrites in a wide spectral range including a charge-transfer band. Figure 5 shows the spectral dependence of the quantity $\Delta\varepsilon = \varepsilon_a - \varepsilon_b$ for the orthoferrite $YFeO_3$, obtained on the basis of the data given in Ref. 20. This figure includes also the results of modeling of this dependence by a set of Lorentzian dispersion curves allowing for the functions F and for their derivatives F'. It should be noted that the values of $\hbar\omega_{0j}$ and Γ_j obtained in the course of fitting of the data for the $^6A_{1g}$–$^6T_{1u}$ allowed transitions are in good agreement with those reported earlier for other orthoferrites.[21] The values of the amplitude factors demonstrate that the main contribution to the natural birefringence of orthoferrites is due to the influence of V_{LCF} on the charge-transfer states. A comparison of the amplitude factors A_j and B_j demonstrates that the contributions of the splitting and mixing to the orthoferrite birefringence are in competition and that their values are in agreement with an estimate of the LCF parameter $B_{\gamma\gamma} \sim 0.1$ eV. The model $\Delta\varepsilon(\omega)$ dependence observed in the long-wavelength range describes well the experimental data of Ref. 22, also plotted in Fig. 5.

4. DISCUSSION OF THE RESULTS OF EXPERIMENTAL MEASUREMENTS OF THE QUADRATIC MAGNETOOPTIC EFFECTS IN $RFeO_3$

A comparative analysis of the experimental results (Figs. 3 and 4) shows that the magnitudes and spectral dependences of $\Delta\varepsilon_{zz}$ are similar for $HoFeO_3$ and $TmFeO_3$, but are quite different from $\Delta\varepsilon_{xx}$ for $TmFeO_3$, indicating an anisotropy of the quadratic magnetooptic effects in orthoferrites. The spectral dependences $\Delta\varepsilon_{zz}(\omega)$ and $\Delta\varepsilon_{xx}(\omega)$ are

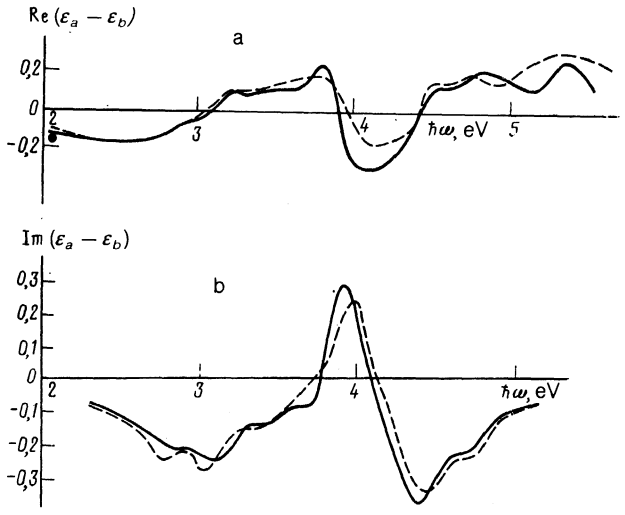

FIG. 5. Frequency dependences of the natural birefringence $\Delta\varepsilon$ of orthoferrite $YFeO_3$. The dashed curve represents the experimental data from Ref. 20; the black dot gives the value taken from Ref. 22; the continuous curves are the results of a model analysis. a) $\mathrm{Re}(\Delta\varepsilon)$; b) $\mathrm{Im}(\Delta\varepsilon)$.

complex and are characterized by a strong dispersion in the region of the charge-transfer band, which is the result of superposition of the contributions of the allowed transitions characterized by wide lines and forbidden transitions with narrow lines. For example, the spectra of the real and imaginary parts of $\Delta\varepsilon_{zz}(\omega)$ obtained for $TmFeO_3$ demonstrate clearly the contribution of the allowed transition characterized by an energy $\hbar\omega_0 = 3.15$ eV (proportional to F'), as well as a fairly strong contribution of a forbidden transition characterized by $\hbar\omega_0 = 2.75$ eV with a spectral dependence representing a combination of F' and F'', which is most probably evidence of the presence of two closely spaced levels at $\hbar\omega_0 = 2.75$ eV.

We analyzed the spectral dependences of the quadratic magnetooptic effects in $TmFeO_3$ using the values of the transition frequencies and line half-widths which were obtained from a quantitative analysis of the linear magnetooptic effects and agreed well with the corresponding values for $YFeO_3$ and $EuFeO_3$ reported in Ref. 21. The results of a model treatment of the spectra of $\Delta\varepsilon_{zz}(\omega)$ for $TmFeO_3$, carried out in the long-wavelength part of the charge-transfer band, are presented in Fig. 4. It should be mentioned that a more detailed analysis of the spectra in the hf range would require a higher (compared with ours) precision of determination of the quantities $\Delta\varepsilon_{ii}(\omega)$.

A calculation of the contribution of the spin–orbit interaction to the quadratic magnetooptic effects is simplest from the theoretical point of view. In this case we have to bear in mind that the mechanism of splitting for the allowed ${}^6A_{1g}-{}^6T_{1u}$ transition contributes to the isotropic relationship of the $\alpha_{ij} = \mathrm{const}\cdot\mathbf{S}_i\mathbf{S}_j$ type between the polarizability and the spins [see Eq. (11)], which cannot account for the anisotropy of the quadratic magnetooptic effects. Moreover, this mechanism is characterized by a spectral dependence proportional to F'', since in the case of the "peak" values of the corresponding contribution to $\Delta\varepsilon_{ii}$ we obtain $\max(\Delta\varepsilon_{ii}) \approx 3\cdot 10^{-6}\lambda^2 f/\Gamma^3$ (λ is in reciprocal centimeters and Γ is in electron volts). If we assume that $\lambda \approx 50\ \mathrm{cm}^{-1}$, $f \approx 0.03$, and $\Gamma \approx 0.4$ eV, which are typical of the first allowed ${}^6A_{1g}-{}^6T_{1u}$ ($\hbar\omega_0 = 3.15$ eV) transition,[21] we obtain a value which is much less than that found experimentally.

An allowance for the effects quadratic in V_{so} in calculation of the contribution made by forbidden charge-transfer transitions gives amplitude factors comparable with the fitting values for the satellites of the allowed transition nearest on the energy scale. The strongest, in respect of $\Delta\varepsilon$, are the transitions ${}^6A_{1g}-{}^6A_{1u}$, ${}^6A_{1g}-{}^6T_{2u}$, ${}^6A_{1g}-{}^6E_u$ (they are given in the decreasing order of intensity). Nevertheless, the allowance for V_{so} cannot, for example, explain the anomalously large contribution to $\Delta\varepsilon_{zz}$ made by a forbidden transition with $\hbar\omega_0 = 2.75$ eV, separated by 0.4 eV from the allowed transition. Therefore, the most probable reason for the special features of the quadratic magnetooptic effects exhibited by orthoferrites in a wide range of frequencies is the magnetooptoelastic mechanism.[11] According to Ref. 11, this mechanism accounts for the characteristics of the magnetic birefringence of $YFeO_3$ associated with the induced spin $\Gamma_4-\Gamma_2$ reorientation at $\lambda = 0.63\ \mu$m. The microscopic nature of the magnetoelastic effect is related to changes in V_{LCF} and V_{exch}, which means it is associated with the changes in the optical anisotropy under the influence of magnetostrictive strains which may be macroscopic (intrinsic magnetostriction) or microscopic (due to latent displacements of sublattices—see Ref. 11). The results of a model analysis of the dependences $\Delta\varepsilon_{zz}(\omega)$ in the case of $TmFeO_3$ are in full agreement with the hypothesis of the predominant role of the magnetoelastooptic mechanism. For example, the values of the amplitude factors for the contributions of allowed transitions to $\Delta\varepsilon_{ii}$ can be used to estimate ΔB_{ii}, which is the change in the effective LCF parameter as a result of the $\Gamma_4-\Gamma_2$ spin reorientation transition in $TmFeO_3$:

$|\Delta B_{xx}| \approx 8\ \mathrm{cm}^{-1}$, $|\Delta B_{zz}| \approx 16\ \mathrm{cm}^{-1}$ (transition $\hbar\omega_0 = 3{,}15$ eV),

$|\Delta B_{xx}| \approx 6\ \mathrm{cm}^{-1}$, $|\Delta B_{zz}| \approx 8\ \mathrm{cm}^{-1}$ (transition $\hbar\omega_0 = 3{,}96$ eV).

These are reasonable values because the strains in the FeO_6^{9-} complexes due to the $\Gamma_4-\Gamma_2$ spin-reorientation transition can reach 10^{-4} (Ref. 14) and the derivatives $\partial B_{ij}/\partial\varepsilon$ become $\sim 10^5\ \mathrm{cm}^{-1}$ (Ref. 11). An estimate of the parameters $B_{ij} \sim 0.1$ eV is obtained allowing for the derivative $\partial B_{ij}/\partial\varepsilon$ and for the presence of structural strains in the FeO_6^{9-} octahedra of the order of 10^{-2} (Ref. 14).

The values of ΔB_{ij} indicate the possibility of a significant contribution to $\Delta\varepsilon_{ii}$ of the quadratic (in respect of $V_{\mathrm{LCF}}^{\mathrm{eff}} = V_{\mathrm{LCF}} + V_{\mathrm{exch}}$) effects occurring in the course of forbidden transitions. The magnetoelastooptic contribution to the appropriate amplitude factors for the ${}^6A_{1g}-{}^{2S+1}\Gamma_u$ transition includes a factor of the type

$$2\langle {}^6T_{1u}|V_{\mathrm{LCF}}^{\mathrm{eff}}|{}^{2S+1}\Gamma_u\rangle\langle {}^{2S+1}\Gamma_u|\Delta V_{\mathrm{LCF}}^{\mathrm{eff}}|{}^6T_{1u}\rangle \sim 2B\Delta B,$$

whereas in the case of the spin-orbit contribution it becomes

$$\langle {}^6T_{1u}|V_{so}|{}^{2S+1}\Gamma_u\rangle\langle {}^{2S+1}\Gamma_u|V_{so}|{}^6T_{1u}\rangle \sim \lambda^2 S^2,$$

so that in the case of some forbidden transitions we can expect competition between both mechanisms. In any case, the lf part of the spectral dependences of the quadratic magnetooptic effects should be governed primarily by the magnetoelastooptic contribution.

5. CONCLUSIONS

The hypothesis of the predominant influence of charge-transfer transitions in the octahedral FeO_6^{9-} complexes on the observed optical and magnetooptic properties of orthoferrites provides reasonable qualitative and quantitative descriptions of the spectral dependences of the quadratic magnetooptic effects in $TmFeO_3$, $HoFeO_3$, and $DyFeO_3$.

An analysis of the experimental results demonstrates a significant role of the mixing mechanism and of the mechanism of splitting of the various ${}^6T_{1u}$ terms of the octahedral complexes, and in some cases it shows that forbidden charge-transfer transitions take place.

Numerical estimates of the contributions of various mechanisms of the quadratic (even) magnetooptic effects and also an analysis of their spectral dependences are evidence of the predominance of the magnetoelastooptic mechanism.

One basic characteristic difference between the quadratic linear magnetooptic effects should be mentioned. In the case of the linear effects it is possible to calculate them from a unified standpoint and the results apply to different paramagnetic and magnetically ordered crystals, because it is possible simply to sum the characteristics of the magnetically active FeO_6^{9-} complexes, whereas the task of calculating the quadratic magnetooptic effects is more difficult. Since the quadratic effects are governed primarily by the internal magnetostriction, i.e., by the displacements of the sublattice ions due to rotation of the magnetization vector, calculation of the quadratic magnetooptic effects requires an individual approach to each type of crystal.

[1] R. V. Pisarev, I. G. Siniĭ, and G. A. Smolenskiĭ, Pis'ma Zh. Eksp. Teor. Fiz. **9**, 294 (1969) [JETP Lett. **9**, 172 (1969)].
[2] V. E. Zubov, G. S. Krinchik, and V. A. Lyskov, Zh. Eksp. Teor. Fiz. **81**, 1489 (1981) [Sov. Phys. JETP **54**, 789 (1981)].
[3] A. S. Borovik-Romanov, N. M. Kreĭnes, and M. A. Talalaev, Pis'ma Zh. Eksp. Teor. Fiz. **13**, 80 (1971) [JETP Lett. **13**, 54 (1971)]; A. S. Borovik-Romanov, N. M. Kreĭnes, A. A. Pankov, and M. A. Talalaev, Zh. Eksp. Teor. Fiz. **66**, 782 (1974) [Sov. Phys. JETP **39**, 378 (1974)].
[4] N. F. Kharchenko, V. V. Eremenko, and O. P. Tutakina, Zh. Eksp. Teor. Fiz. **64**, 1326 (1973) [Sov. Phys. JETP **37**, 672 (1973)].
[5] A. S. Borovik-Romanov, N. M. Kreĭnes, A. A. Pankov, and M. A. Talalaev, Zh. Eksp. Teor. Fiz. **64**, 1762 (1973) [Sov. Phys. JETP **37**, 890 (1973)].
[6] J. Ferre and G. A. Gehring, Rep. Prog. Phys. **47**, 513 (1984).
[7] G. S. Krinchik and G. K. Tyutneva, Zh. Eksp. Teor. Fiz. **46**, 435 (1964) [Sov. Phys. JETP **19**, 292 (1964)].
[8] G. S. Grinchik, V. D. Gorbunova, V. S. Gushchin, and A. A. Kostyurin, Zh. Eksp. Teor. Fiz. **78**, 869 (1980) [Sov. Phys. JETP **51**, 435 (1980)]; G. S. Krinchik, A. A. Kostyurin, V. D. Gorbunova, and V. S. Gushchin, Zh. Eksp. Teor. Fiz. **81**, 1037 (1981) [Sov. Phys. JETP **54**, 550 (1981)].
[9] J. C. Suits and B. E. Argyle, Phys. Rev. Lett. **14**, 687 (1965).
[10] B. B. Krichevtsov, R. V. Pisarev, and M. M. Ruvinshteĭn, Fiz. Tverd. Tela (Leningrad) **22**, 2128 (1980) [Sov. Phys. Solid State **22**, 1240 (1980)].
[11] A. S. Moskvin, D. G. Latypov, and V. G. Gudkov, Fiz. Tverd. Tela (Leningrad) **30**, 413 (1988) [Sov. Phys. Solid State **30**, 235 (1988)].
[12] J. F. Dillon Jr., J. P. Remeika, and C. R. Staton, J. Appl. Phys. **41**, 4613 (1970).
[13] Yu. P. Gaĭdukov, A. V. Zenkov, S. V. Koptsik *et al.*, Pis'ma Zh. Eksp. Teor. Fiz. **51**, 201 (1990) [JETP Lett. **51**, 228 (1990)].
[14] K. P. Belov, A. K. Zvezdin, A. M. Kadomtseva, and R. Z. Levitin, *Orientational Transitions in Rare-Earth Magnetic Materials* [in Russian], Nauka, Moscow (1979).
[15] G. A. Bolotin, Fiz. Met. Metalloved. **39**, 731 (1975).
[16] R. V. Pisarev, Zh. Eksp. Teor. Fiz. **58**, 1421 (1970) [Sov. Phys. JETP **31**, 761 (1970)].
[17] N. F. Kharchenko and S. L. Gnatchenko, Fiz. Nizk. Temp. **7**, 475 (1981) [Sov. J. Low Temp. Phys. **7**, 234 (1981)].
[18] A. I. Likhtenshtein, A. S. Moskvin, and V. A. Gubanov, Fiz. Tverd. Tela (Leningrad) **24**, 3596 (1982) [Sov. Phys. Solid State **24**, 2049 (1982)].
[19] L. D. Landau, E. M. Lifshitz, and M. P. Pitaevskiĭ, *Electrodynamics of Continuous Media*, 2nd ed., Pergamon Press, Oxford (1984).
[20] S. Visnovsky, B. M. Wanklyn, and V. Prosser, IEEE Trans. Magn. **MAG-20**, 1054 (1984).
[21] A. V. Zenkov, E. A. Gan'shina, and S. V. Koptsik *et al.*, Deposited Paper No. 788-V90 [in Russian], VINITI, Moscow (1990).
[22] L. Jastrzębski, Phys. Status Solidi A **21**, 57 (1974).

Translated by A. Tybulewicz